Anti-Icing Surfaces

Subjects: Materials Science, Coatings & Films
Contributor: Annalisa Volpe

In numerous fields such as aerospace, the environment, and energy supply, ice generation and accretion represent a severe issue. For this reason, numerous methods have been developed for ice formation to be delayed and/or to inhibit ice adhesion to the substrates. Among them, laser micro/nanostructuring of surfaces aiming to obtain superhydrophobic behavior has been taken as a starting point for engineering substrates with anti-icing properties.

Keywords: anti-icing ; laser ; microstructuring ; wettability ; superhydrophobicity ; metals ; polymers

1. Introduction

Ice in its several forms, i.e., frost, glaze, rime, snow, can cause severe problems for locks and dams [1], solar panels [2], wind turbines [3], aircraft [4][5], heat pumps [6], power lines or telecommunication equipment [7], civil engineering materials [8], and oil platforms [9], especially when it adheres and accumulates. These problems can increase energy consumption, reduce the energy conversion efficiency, origin mechanical and/or electrical malfunctions, and define safety hazards [10] [11]. Among all the mentioned fields, the aerospace industry is particularly affected by icing phenomena, which can occur both while aircraft are on the ground [12] and in the air [13]. In the first case, before flying, ice needs to be removed, since it alters aerodynamic properties, and ice fragments can be sheared off by aerodynamic drag and fly into the engines. In the latter case, the impact of supercooled water droplets found in clouds, depending on atmospheric conditions, may stick to the surface, creating a dangerous ice layer. Therefore, the overall recommendation of the safety authorities is to strengthen the ice protection systems (IPS) to all commercial aircraft [14]. These protection systems can be classified into two groups: anti-icing systems, which aim to prevent ice formation, and de-icing systems, which aim at the removal of already-accumulated ice or frost from a surface.

In recent years, great attention has been paid to the anti-icing surfaces, as attested by the increasing number of research papers and patents related to the topic "anti-icing" (Figure 1).

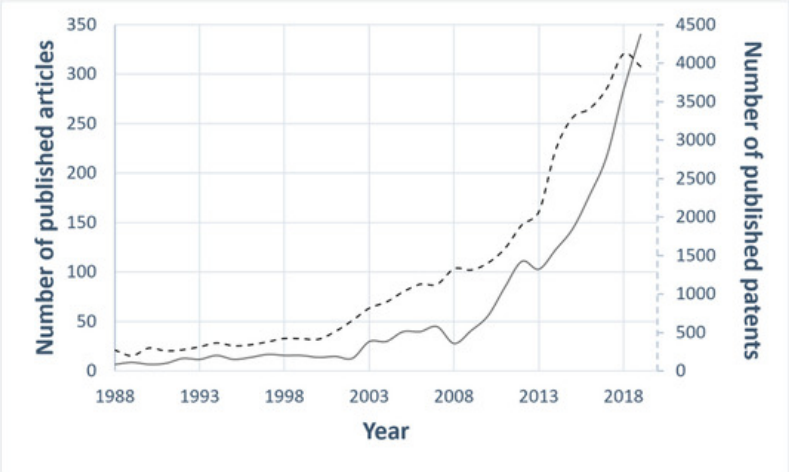

Figure 1. The statistics of the published articles indexed in Scopus (black line) and of the published patents listed in Espacenet [15] (black dotted line) on the topic of "anti-icing". Year range selected: 1988–2019.

It can be difficult to find a common definition of anti-icing, but some ubiquitous features must be exhibited by such surfaces, i.e., (i) inhibition of water condensation on the surface; (ii) inhibition of the incoming water's freezing; and (iii) weakening of the adhesion strength of ice, when formed, so that it can be easily removed [16].

Different strategies have been employed to prevent ice accretion and to easily remove it, and they can be divided into active and passive approaches.

Keeping the surface temperature above the freezing point by means of electro-thermal heating is an efficient active method to reduce the likelihood of ice formation or to enhance its melting [17]. The exploitation of the Joule effect for heating line conductors is at present recognized as the most efficient engineering approach [18], especially in the case of transmission lines. However, this strategy is extremely time and energy consuming. In addition, electromagnetic disturbance can be generated by the passage of electric flow, which could interfere with the operation of the apparatus. Another method is to use freezing point depressants. It is well known that salt depresses the freezing point to the eutectic point, facilitating the ice in melting. Instead, in order to prevent icing and frosting of water on aircrafts surfaces, organic liquids are exploited, thanks to their lower crystallization temperatures compared to plain water [13]. In particular, for commercial aircraft in the northern hemisphere, various de-icing fluids are used [12][19]. They are essential not just on the exposed surfaces of aircraft wings, but also on other aerodynamic areas such as under the wings and on the rear spar stabilizer areas. Two standard test methods, namely Wet Spray Endurance Test [20] and Boundary Layer Displacement Thickness [21] are employed in climatically controlled wind tunnels to give a measure of the remaining film thickness on a surface during its continuous removal under an increasing flow of air over it. Both tests are critical for safe flight operation and are closely associated with density, surface tension and viscosity of the exploited fluids.

This notwithstanding, the use of chemical agents to prevent ice formation has many drawbacks. First, their effectiveness is short-lived. Therefore, for large surfaces, periodic treatments are required. Furthermore, extensive use of these liquids, besides having high costs, can cause environmental problems [22].

Other active de-icing techniques consist of using mechanical forces to remove ice accretion from surfaces. With this aim, direct scraping or mechanical removal by shock waves, vibrations, or the twisting of conductors are applied. However, these methods often require personnel to reach the lines and towers; furthermore, helicopters or even shotguns must also be exploited when the ice is less accessible [18]. Moreover, applying mechanical force during de-icing causes additional stress to the networks, which in some cases can lead to failure. Consequently, such methods are certainly neither safe nor efficient. In addition, many other anti-icing and deicing methods have been studied and applied, e.g., electro-impulse systems, shape memory alloys, and ultrasound technology [23].

In addition, hybrid solutions consisting of material with a combination of passive anti-icing and active deicing functionalities have also been reported [24]. In [25], the prevention of freezing above −14 °C without any source of power input was claimed in the case of incoming water by using a spray-coating of perfluorododecylated graphene nanoribbons (FDO-GNRs), whereas resistive heating represents an alternative active deicing method in more extreme sub-zero environmental conditions.

Thus, most of the active or hybrid strategies striving against ice formation are apparently inefficient, energy-consuming, expensive, or dangerous to the environment. It is thus crucial to develop innovative, green, cost-effective, and efficient technologies for anti-icing and deicing [11].

A new development perspective for pure passive anti-icing methods is surface micro- and nano-structuring. Recently, several efforts have been devoted towards the modification of surface topography and/or chemistry in order to obtain superhydrophobic properties [26][27]. A close relationship between the water repellency of superhydrophobic surfaces (SHSs) and icephobicity has been demonstrated [28]. Indeed, the air trapped between the water droplets and the underlying surface texture allows the surfaces to exhibit not only high water contact angle (WCA) and low contact angle (CA) hysteresis [29], but also prevent ice formation because of reduced water adhesion. Consequently, using SHSs for anti-icing application is undoubtedly an inherently attractive strategy. Among the different technologies available for surface micro- and nano-structuring, short and ultrashort laser pulses have several advantages: (i) they offer extreme flexibility in the morphology of the structures and surface micro-/nano-features that can be created [30][31][32][33]; (ii) in principle, they have no limitations in terms of manufacturable materials, as long as the targets absorb the laser wavelength [34][35]; and (iii) it is possible to scale up such technology [36] to structure large areas with industrially relevant process times and costs [37].

2. Surface Wettability

2.1. Key Concepts

Wettability is the result of the stability of the three phases, i.e., gas, liquid and solid, which come into play when a liquid lies on a solid surface. In fact, while the force at the solid–liquid interface (adhesive) tends to spread the liquid, that within the liquid itself (cohesive) instead resists spreading. Therefore, the balance between such forces determines the ability of the surface to be wet. The wetting behavior is normally evaluated by considering the contact angle (CA), i.e., the angle θ between a droplet deposited on the surface and the surface itself, as shown in Figure 2.

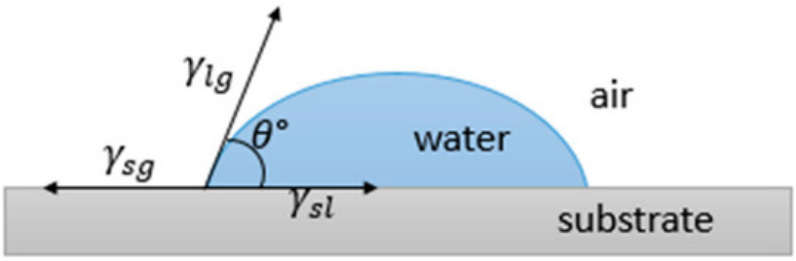

Figure 2. Contact angle of a liquid lying on a surface and balance between surface tensions.

In the early nineteenth century, Young found a relationship relating the intrinsic contact angle θ to the surface tensions of the liquid–gas *ylg*, solid–gas *ysg*, and solid–liquid interfaces *ysl*, which can be expressed as [38]:

$$\gamma_{sl} = \gamma_{sg} - \gamma_{lg} cos\theta \quad (1)$$

This relation, also called the Young equation, is the starting point for all the investigation on the wetting behavior of surfaces.

As mentioned before, another important concept to be introduced to investigate the wettability is the adhesion of the water droplet to the substrate, addressable through the work of adhesion *Wa* [39]. This can be defined as the work done when two surfaces are separated to a distance of infinity and, in case of liquid–solid combinations, can be expressed as:

$$W_a = \gamma_{sg} + \gamma_{lg} - \gamma_{sl} \quad (2)$$

From (1) and (2), *W*a can be also expressed as:

$$W_a = \gamma_{lg} (1 + cos\theta) \quad (3)$$

A low contact angle (θ<90°) indicates hydrophilicity, namely good wetting. If the angle approaches zero, *Wa*=2*ylg*, and total wetting is observed with the formation of a liquid film. When θ>90°, hydrophobic properties are revealed, while for θ>150°, the surface is classed as superhydrophobic. No wetting and no adhesion are instead characteristics of a surface where θ=180°, that is, *Wa* becomes zero.

For non-ideal surfaces, where non-homogenous chemical composition and/or non-uniform topography are present, wettability cannot be described by Equation (1). Consequently, the apparent contact angle $\theta*$ [40] is considered instead of θ. Considering real solid rough surface, two possible configurations can be sketched for a deposited droplet: (i) it adapts to the contours of the real solid surface, conforming to the peaks and valleys of its roughness (Wenzel state, Figure 3a); or (ii) it stands on the nails of the roughness, leaving only air to fill the cavities below (Figure 3b). This latter condition, the Cassie and Baxter state, is also called the "fakir" state, since the droplet lies on micro asperities [41].

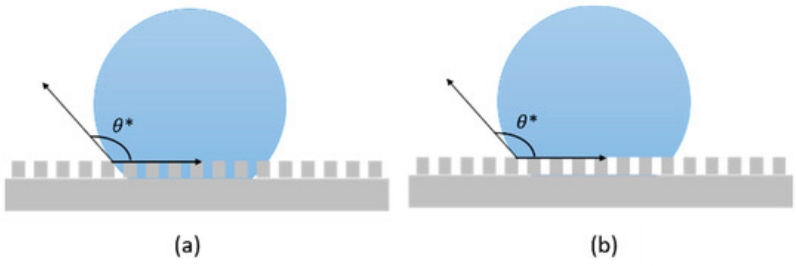

Figure 3. Schematic of droplet in (**a**) Wenzel state and (**b**) Cassie and Baxter state.

In the Wenzel state, the apparent CA depends on the Young's CA through the Wenzel wetting equation [42]:

$$cos\theta^* = r\, cos\theta \quad (4)$$

where r is ≥1, and it is defined as [42]:

$$r = \text{rouhgness factor} = \frac{\text{actual surface}}{\text{geometrical surface}} \quad (5)$$

namely, the ratio of the effective solid surface area to the apparent projection area of a rough surface [43].

The Wenzel Equation (4), perfectly suitable for characterizing hydrophilic and hydrophobic surfaces, reveals that the contact angle $\theta*$ of a real surface can be increased by increasing its roughness. Nevertheless, this model fails to describe superhydrophobicity, because it does not consider the air pockets that are bounded between the surface and liquid. Consequently, another model was introduced to explain many wetting phenomena, such as the lotus effect [44] and self-cleaning behavior [45], obtainable when CA>150 °, developed by Cassie and Baxter.

In case of superhydrophobicity, the droplet no longer infiltrates the surface roughness, but a kind of combined phase contact is established between the solid–liquid and gas–liquid interfaces. So they introduced a new relationship for the apparent contact angle [46]:

$$cos\theta^* = f_1 cos\theta_1 + f_2 cos\theta_2 \quad (6)$$

where $\theta 1$ and $\theta 2$ are, respectively, the Young contact angles of the liquid droplet on the solid and gas bearings, while $f1$ and $f2$ are the percentage of the solid–liquid and gas–liquid contact area, with $f1+f2=1$. Therefore, if $\theta 2=180°$, Equation (6) becomes:

$$cos\theta^* = f_1\, cos\theta_1 + f_1 - 1 \quad (7)$$

which explains some non-wetting superhydrophobic phenomena [47]. The existence of a critical value of roughness factor was found to dictate the transition between the two mentioned wetting states, as found Dettre and Johnson, who stated that beyond it, wettability is better described by the Cassie–Baxter model than by Wenzel [48].

Besides the apparent contact angle $\theta*$, contact angle hysteresis (CAH) gives valuable information on the moving properties of a droplet on a solid surface [49]. When a surface is inclined, an advancing and a receding front, forming different angles with the surface, can be recognized as the droplet slides. The difference $\Delta\theta$ between these two angles, the advancing θA and the receding θR (Figure 4), defines the CAH. When $\Delta\theta<10°$, the droplet can be easily removed from the surface; conversely, when $\Delta\theta$ is sufficiently large, the liquid viscosity is such that the droplet cannot readily roll off the surface.

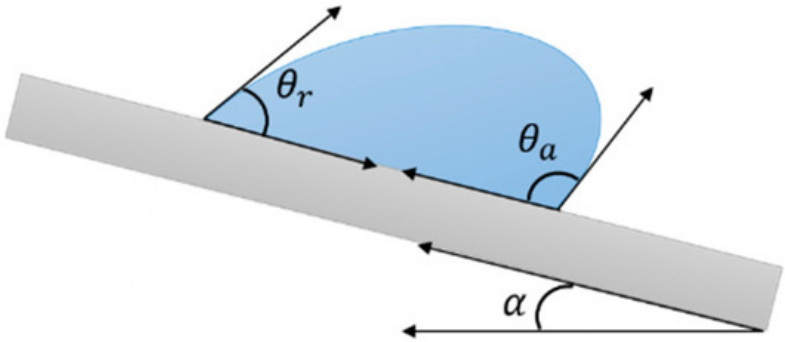

Figure 4. Schematic of advancing and receding angles of a droplet sliding on a surface. Contact angle hysteresis is defined as the difference between these two.

Another angle that characterizes a moving droplet is the rolling angle α (see Figure 4), also called roll-off angle or sliding angle SA, namely, the minimum angle at which a liquid droplet would begin to slide down an inclined surface. It is related to several factors, such as CA, CAH and droplet size [50][51], and can be described by the following equation, where the sliding angle is defined depending on the advancing and receding contact angles (θa and θr, respectively) [52]:

$$sin\alpha = \frac{\gamma Rk}{mg}(cos\theta_r - cos\theta_a) \quad (8)$$

where γ is the surface tension, R and k are length scale and shape constants for describing the droplet profile (R is generally taken to be the drop radius, while k is an empirical parameter obtained by fitting the experimental data), respectively, m is the mass of the droplet, and g is the gravitational acceleration. Thus, a small hysteresis corresponds to a small SA, and researchers usually correlate water adhesion to CHA or SA interchangeably.

Usually, the total wetting Wenzel regime characterizes sticky surfaces with high CAH, where the water droplets tend to grip more than to a flat equivalent surface. Conversely, surfaces which behave in the Cassie and Baxter state are slippery and are characterized by a low CAH, which leads the water drop to slide away more easily than an equivalent flat surface. However, the existence of "sticky" surfaces, i.e., with high intrinsic contact angle hysteresis, in the regime of Cassie and Baxter has also been reported [53][54].

3. Anti-Icing Properties

In recent years, scientists have found that a key factor to obtaining anti-icing properties is superhydrophobicity, which can be obtained through low surface energy coatings [55] or by increasing the surface roughness [56][57][58]. Dwelling on the latter strategy, the bio-inspired example of SHS, such as surfaces reproducing the doubled micro-nanostructures of the lotus leaf, have attracted great attention [59][60][61][62][63].

Tourkine et al. showed that using SHS at subzero temperature made it possible to easily remove a deposited water drop before freezing thanks solely to gravity, thus preventing the formation of an ice layer [64]. Furthermore, Kulinich et al. [29] suggested that only when the CAH was low would the correspondence between low ice adhesion and high CA be consistent, suggesting icephobicity to be related to the CAH rather than to superhydrophobicity alone. Indeed, higher CAH indicates higher water–solid adhesion and, consequently, at subzero temperature, when the water becomes ice, higher ice adhesion, too. On the contrary, water-repellent surfaces, i.e., those that exhibit high water CAs and low CAHs, remain dry because of the easy water roll off, and thus, at subzero temperature, ice-formation is reduced.

The main aspects investigated to assess the anti-icing properties of a surface are:

- icing delay, intended both as a time delay in the solidification of the water and as a reduction in the threshold temperature for freezing. A lower threshold for the formation of ice would, indeed, allow wider range of operating temperature conditions. Similarly, a postponement of freezing would increase the probability of water removal before solidification.
- interaction between water and the solid surface. That is, if before freezing occurs, water droplets were to roll off the surface, there would be no chance of ice being formed. This phenomenon is strictly correlated with the sliding angle.
- ice adhesion. Although ice is formed, its adhesion should be minimized, so that a small external force or, e.g., in case of a wind turbine, the centrifugal force of its own blades, is sufficient to remove the frozen layer, facilitating the de-icing process.

Usually, the testing of these three aspects of an anti-icing surface takes place at atmospheric pressure and in static conditions. Consequently, in the aerospace field, these tests are more appropriate for verifying the anti-icing formation on the ground than in the air, where the atmospheric conditions are more extreme.

References

1. Frankenstein, S.; Tuthill, A.M. Ice adhesion to locks and dams: Past work; future directions? J. Cold Reg. Eng. 2002, 16, 83–96, doi:10.1061/(ASCE)0887-381X(2002)16:2(83).
2. Fillion, R.M.; Riahi, A.R.; Edrisy, A. A review of icing prevention in photovoltaic devices by surface engineering. Renew. Sustain. Energy Rev. 2014, 32, 797–809, doi:10.1016/j.rser.2014.01.015.
3. Parent, O.; Ilinca, A. Anti-icing and de-icing techniques for wind turbines: Critical review. Cold Reg. Sci. Technol. 2011, 65, 88–96, doi:10.1016/j.coldregions.2010.01.005.
4. Lynch, F.T.; Khodadoust, A. Effects of ice accretions on aircraft aerodynamics. Prog. Aerosp. Sci. 2001, 37, 669–767, doi:10.1016/S0376-0421(01)00018-5.
5. Vercillo, V.; Karpen, N.; Laroche, A.; Mayén Guillén, J.A.; Tonnicchia, S.; de Andrade Jorge, R.; Bonaccurso, E. Analysis and modelling of icing of air intake protection grids of aircraft engines. Cold Reg. Sci. Technol. 2019, 160, 265–272, doi:10.1016/j.coldregions.2019.01.012.
6. Song, M.; Dong, J.; Wu, C.; Jiang, Y.; Qu, M. Improving the frosting and defrosting performance of air source heat pump units: Review and outlook. HKIE Trans. Hong Kong Inst. Eng. 2017, 24, 88–98, doi:10.1080/1023697X.2017.1313134.
7. Laforte, J.L.; Allaire, M.A.; Laflamme, J. State-of-the-art on power line de-icing. Atmos. Res. 1998, 46, 143–158, doi:10.1016/S0169-8095(97)00057-4.

8. Xiang, T.; Lv, Z.; Wei, F.; Liu, J.; Dong, W.; Li, C.; Zhao, Y.; Chen, D. Superhydrophobic civil engineering materials. Coatings 2019, 9, 753.
9. Ryerson, C.C. Ice protection of offshore platforms. Cold Reg. Sci. Technol. 2011, 65, 97–110, doi:10.1016/j.coldregions.2010.02.006.
10. Fang, Y.; Yong, J.; Chen, F.; Huo, J.; Yang, Q.; Zhang, J.; Hou, X. Bioinspired fabrication of Bi/Tridirectionally anisotropic sliding superhydrophobic PDMS surfaces by femtosecond laser. Adv. Mater. Interfaces 2018, 5, 1–8, doi:10.1002/admi.201701245.
11. Lv, J.; Song, Y.; Jiang, L.; Wang, J. Bio-inspired strategies for anti-icing. ACS Nano 2014, 8, 3152–3170.
12. Kotker, D. Training Recommendations and Background Information for De-Icing /Anti-Icing of Aeroplane on the Ground; Technical Report for AEA Publications: Pittsburgh, PA, USA, August 2015
13. Thomas, S.K.; Cassoni, R.P.; MacArthur, C.D. Aircraft anti-icing and de-icing techniques and modeling. J. Aircr. 1996, 33, 841–854, doi:10.2514/3.47027.
14. Alamri, S.; Vercillo, V.; Aguilar-Morales, A.I.; Schell, F.; Wetterwald, M.; Lasagni, A.F.; Bonaccurso, E.; Kunze, T. Self-limited ice formation and efficient de-icing on superhydrophobic micro-structured airfoils through direct laser interference patterning. Adv. Mater. Interfaces 2020, 2001231, 1–10, doi:10.1002/admi.202001231.
15. Available online: https://worldwide.espacenet.com/patent/ (accessed on 7 December 2020).
16. Hejazi, V.; Sobolev, K.; Nosonovsky, M. From superhydrophobicity to icephobicity: Forces and interaction analysis. Sci. Rep. 2013, 3, 2194, doi:10.1038/srep02194.
17. Vertuccio, L.; De Santis, F.; Pantani, R.; Lafdi, K.; Guadagno, L. Effective de-icing skin using graphene-based flexible heater. Compos. Part B Eng. 2019, 162, 600–610, doi:10.1016/j.compositesb.2019.01.045.
18. Farzaneh, M.; Volat, C.; Leblond, A. Anti-icing and de-icing techniques for overhead lines. Atmos. Icing Power Netw. 2008, 229–268, doi:10.1007/978-1-4020-8531-4_6.
19. Hille, J. Boeing deicing and anti-icing fluid residues. Boeing 2007, 25, 14–21.
20. Water Spray and High Humidity Endurance Test Methods for AMS1424 and AMS1428 Aircraft Deicing/Anti-Icing Fluids AS5901D; Society of Automotive Engineers International: Warrendale, PA, USA, 2019, doi:https://doi.org/10.4271/AS5901D
21. Standard Test Method for Aerodynamic Acceptance of SAE AMS1424 and SAE AMS1428 Aircraft Deicing/Anti-icing Fluids; Society of Automotive Engineers International: Warrendale, PA, USA, 2016.
22. Yong, J.S. Evaluation of the Environmental Impacts and Alternative Technologies of Deicing/Anti-Icing Operations at Airports. Ph.D. Thesis, University of Illinois at Urbana Champaign, Champaign, IL, USA, 2001.
23. Goraj, Z. An overview of the deicing and antiicing technologies with prospects for the future. In Proceedings of the 24th International Congress of the Aeronautical Sciences, 29 August–3 September 2004; ICAS: Yokohama, Japan, 2004; pp. 1–11.
24. Huang, X.; Tepylo, N.; Pommier-budinger, V.; Budinger, M.; Villedieu, P.; Bennani, L.; Huang, X.; Tepylo, N.; Pommier-budinger, V.; Budinger, M.; et al. A survey of icephobic coatings and their potential use in a hybrid coating/active ice protection system for aerospace applications To cite this version: HAL Id: Hal-02024879. Prog. Aerosp. Sci. 2019, 105, 74–97.
25. Wang, T.; Zheng, Y.; Raji, A.R.O.; Li, Y.; Sikkema, W.K.A.; Tour, J.M. Passive anti-icing and active deicing films. ACS Appl. Mater. Interfaces 2016, 8, 14169–14173, doi:10.1021/acsami.6b03060.
26. Simpson, J.T.; Hunter, S.R.; Aytug, T. Superhydrophobic materials and coatings: A review. Rep. Prog. Phys. 2015, 78, 86501, doi:10.1088/0034-4885/78/8/086501.
27. Shirtcliffe, N.J.; McHale, G.; Atherton, S.; Newton, M.I. An introduction to superhydrophobicity. Adv. Colloid Interface Sci. 2010, 161, 124–138, doi:10.1016/j.cis.2009.11.001.
28. Esmeryan, K.D. From extremelywater-repellent coatings to passive icing protection-principles, limitations and innovative application aspects. Coatings 2020, 10, 1–20, doi:10.3390/coatings10010066.
29. Kulinich, S.A.; Farzaneh, M. How wetting hysteresis influences ice adhesion strength on superhydrophobic surfaces. Langmuir 2009, 25, 8854–8856, doi:10.1021/la901439c.
30. Volpe, A.; Paiè, P.; Ancona, A.; Osellame, R. Polymeric fully inertial lab-on-a-chip with enhanced-throughput sorting capabilities. Microfluid. Nanofluidics 2019, 23, 37, doi:10.1007/s10404-019-2206-1.
31. Ancona, A.; Joshi, G.S.; Volpe, A.; Scaraggi, M.; Lugarà, P.M.; Carbone, G. Non-uniform laser surface texturing of an un-tapered square pad for tribological applications. Lubricants 2017, 5, doi:10.3390/lubricants5040041.

32. Ancona, A.; Carbone, G.; De Filippis, M.; Volpe, A.; Lugarà, P.M. Femtosecond laser full and partial texturing of steel surfaces to reduce friction in lubricated contact. Adv. Opt. Technol. 2014, 3, doi:10.1515/aot-2014-0045.

33. Putignano, C.; Parente, G.; Profito, F.J.; Gaudiuso, C.; Ancona, A.; Carbone, G. Laser microtextured surfaces for friction reduction: Does the pattern matter? Materials 2020, 13, 1–21, doi:10.3390/ma13214915.

34. Gaudiuso, C.; Volpe, A.; Ancona, A. One-step femtosecond laser stealth dicing of quartz. Micromachines 2020, 1, 327.

35. Putignano, C.; Scarati, D.; Gaudiuso, C.; Di Mundo, R.; Ancona, A.; Carbone, G. Soft matter laser micro-texturing for friction reduction: An experimental investigation. Tribol. Int. 2019, 136, 82–86, doi:10.1016/j.triboint.2019.03.001.

36. Trotta, G.; Vázquez, R.M.; Volpe, A.; Modica, F.; Ancona, A.; Fassi, I.; Osellame, R. Disposable optical stretcher fabricated by microinjection moulding. Micromachines 2018, 9, doi:10.3390/mi9080388.

37. Giannuzzi, G.; Gaudiuso, C.; Franco, C. Di; Scamarcio, G.; Lugarà, P.M.; Ancona, A. Large area laser-induced periodic surface structures on steel by bursts of femtosecond pulses with picosecond delays. Opt. Lasers Eng. 2019, 114, 15–21, doi:10.1016/j.optlaseng.2018.10.006.

38. Butt, H.J.; Golovko, D.S.; Bonaccurso, E. On the derivation of young's equation for sessile drops: Nonequilibrium effects due to evaporation. J. Phys. Chem. B 2007, 111, 5277–5283, doi:10.1021/jp065348g.

39. Menini, R.; Ghalmi, Z.; Farzaneh, M. Cold regions science and technology highly resistant icephobic coatings on aluminum alloys. Cold Reg. Sci. Technol. 2011, 65, 65–69, doi:10.1016/j.coldregions.2010.03.004.

40. Bormashenko, E. Physics of solid-liquid interfaces: From the young equation to the superhydrophobicity. Low Temp. Phys. 2016, 42, 622–635, doi:10.1063/1.4960495.

41. Jamil, M.I.; Ali, A.; Haq, F.; Zhang, Q.; Zhan, X.; Chen, F.; Jamil, M.I.; Ali, A.; Haq, F.; Zhang, Q.; et al. Icephobic strategies and materials with superwettability: Design principles and mechanism. Langmuir 2018, doi:10.1021/acs.langmuir.8b03276.

42. Wenzel, R.N. Resistance of solid surfaces to wetting by water. Ind. Eng. Chem. 1936, 28, 988–994, doi:10.1021/ie50320a024.

43. Hongru, A.; Xiangqin, L.; Shuyan, S.; Ying, Z.; Tianqing, L. Measurement of Wenzel roughness factor by laser scanning confocal microscopy. RSC Adv. 2017, 7, 7052–7059, doi:10.1039/c6ra26897h.

44. Marmur, A. The lotus effect: Superhydrophobicity and metastability. Langmuir 2004, 20, 3517–3519, doi:10.1021/la036369u.

45. Liu, K.; Jiang, L. Bio-inspired self-cleaning surfaces. Annu. Rev. Mater. Res. 2012, 42, 231–263, doi:10.1146/annurev-matsci-070511-155046.

46. Cassie, A.B.D.; Baxter, S. Wettability of porous surfaces. Trans. Faraday Soc. 1944, 40, 546–551, doi:10.1039/tf9444000546.

47. Lafuma, A.; Quéré, D. Superhydrophobic states. Nat. Mater. 2003, 2, 457–460, doi:10.1038/nmat924.

48. Johnson, R.E.J.; Dettre, R.H. Contact angle hysteresis: Study of an idealized rough surface. In Contact Angle, Wettability, and Adhesion; American Chemical Society: Washington, DC, USA, 1964; pp. 112–135.

49. Olsen, D.A.; Joyner, P.A.; Olson, M.D. The sliding of liquid drops on solid surfaces. J. Phys. Chem. 1962, 66, 883–886, doi:10.1021/j100811a029.

50. Yoshimitsu, Z.; Nakajima, A.; Watanabe, T.; Hashimoto, K. Effects of surface structure on the hydrophobicity and sliding behavior of water droplets. Langmuir 2002, 18, 5818–5822, doi:10.1021/la020088p.

51. Pierce, E.; Carmona, F.J.; Amirfazli, A. Understanding of sliding and contact angle results in tilted plate experiments. Colloids Surf. A Phys. Eng. Asp. 2008, 323, 73–82, doi:10.1016/j.colsurfa.2007.09.032.

52. Fumridge, C.G.L. Studies at phase interfaces I. The sliding of liquid drops on solid surfaces and a theory for spray retention. J. Colloid Sci. 1962, 17, 309–324, doi:10.1016/j.ultrasmedbio.2012.04.007.

53. Quére, D.; Lafuma, A.; Bico, J. Slippy and sticky microtextured solids. Nanotechnology 2003, 14, 1109–1112, doi:10.1088/0957-4484/14/10/307.

54. Giannuzzi, G.; Gaudiuso, C.; Di Mundo, R.; Mirenghi, L.; Fraggelakis, F.; Kling, R.; Lugarà, M. Pietro; Ancona, A. Short and long term surface chemistry and wetting behaviour of stainless steel with 1D and 2D periodic structures induced by bursts of femtosecond laser pulses. Appl. Surf. Sci. 2019, 494, 1055–1065, doi:10.1016/j.apsusc.2019.07.126.

55. Zhu, K.; Li, X.; Su, J.; Li, H.; Zhao, Y.; Yuan, X. Improvement of anti-icing properties of low surface energy coatings by introducing phase-change microcapsules. Polym. Eng. Sci. 2018, 58, 973–979, doi:10.1002/pen.24654.

56. Varanasi, K.K.; Deng, T.; Smith, J.D.; Hsu, M.; Bhate, N. Frost formation and ice adhesion on superhydrophobic surfaces. Appl. Phys. Lett. 2010, 97, doi:10.1063/1.3524513.

57. Mishchenko, L.; Hatton, B.; Bahadur, V.; Taylor, J.A.; Krupenkin, T.; Aizenberg, J. Design of ice-free nanostructured impacting water droplets. ACS Nano 2010, 4, 7699–7707.
58. He, M.; Li, H.; Wang, J.; Song, Y. Superhydrophobic surface at low surface temperature. Appl. Phys. Lett. 2011, 98, 2011–2014, doi:10.1063/1.3558911.
59. Sun, T.; Feng, L.; Gao, X.; Jiang, L. Bioinspired surfaces with special wettability. Acc. Chem. Res. 2005, 38, 644–652.
60. Yao, X.; Song, Y.; Jiang, L. Applications of bio-inspired special wettable surfaces. Adv. Mater. 2011, 23, 719–734, doi:10.1002/adma.201002689.
61. Jagdheesh, R.; Diaz, M.; Oca, J.L. Bio inspired self-cleaning ultrahydrophobic aluminium surface by laser processing. RSC Adv. 2016, 6, 72933–72941, doi:10.1039/C6RA12236A.
62. Groenendijk, M. Fabrication of super hydrophobic surfaces by fs laser pulses. Laser Tech J. 2008, 5, 44–47, doi:10.1002/latj.200890025.
63. Roach, P.; Shirtcliffe, N.J.; Newton, M.I. Progess in superhydrophobic surface development. Soft Matter 2008, 4, 224, doi:10.1039/b712575p.
64. Tourkine, P.; Merrer, M. Le; Quéré, D. Delayed freezing on water repellent materials. Langmuir 2009, 25, 7214–7216, doi:10.1021/la900929u.